Distinct Kondo Screening Behaviors in Heavy Fermion Filled Skutterudites with $4f^1$ and $4f^2$ Configurations

X. Lou,[1] T. L. Yu,[1] Y. H. Song,[1] C. H. P. Wen,[1] W. Z. Wei,[1] A. Leithe-Jasper,[2] Z. F. Ding,[1] L. Shu,[1,3] S. Kirchner,[4,5] H. C. Xu,[1,3,*] R. Peng,[1,3,†] and D. L. Feng[3,6,7,‡]

[1]*Laboratory of Advanced Materials, State Key Laboratory of Surface Physics, and Department of Physics, Fudan University, Shanghai 200438, China*

[2]*Max-Planck-Institut für Chemische Physik fester Stoffe, Nöthnitzer Straβe 40, 01187 Dresden, Germany*

[3]*Shanghai Research Center for Quantum Sciences, Shanghai 201315, China*

[4]*Zhejiang Institute of Modern Physics and Department of Physics, Zhejiang University, Hangzhou 310027, China*

[5]*Zhejiang Province Key Laboratory of Quantum Technology and Device, Zhejiang University, Hangzhou 310027, China*

[6]*Collaborative Innovation Center of Advanced Microstructures, Nanjing 210093, China*

[7]*Hefei National Laboratory for Physical Science at Microscale, CAS Center for Excellence in Quantum Information and Quantum Physics, and Department of Physics, University of Science and Technology of China, Hefei 230026, China*

(Received 8 June 2020; accepted 25 February 2021; published 1 April 2021)

$CeOs_4Sb_{12}$ (COS) and $PrOs_4Sb_{12}$ (POS) are two representative compounds that provide the ideal vantage point to systematically study the physics of multi-f-electron systems. COS with Ce $4f^1$, and POS with Pr $4f^2$ configurations show distinct properties of Kondo insulating and heavy fermion superconductivity, respectively. We unveiled the underlying microscopic origin by angle-resolved photoemission spectroscopy studies. Their eV-scale band structure matches well, representing the common characters of conduction electrons in ROs_4Sb_{12} systems (R = rare earth). However, f electrons interact differently with conduction electrons in COS and POS. Strong hybridization between conduction electrons and f electrons is observed in COS with band dependent hybridization gaps, and the development of a Kondo insulating state is directly revealed. Although the ground state of POS is a singlet, finite but incoherent hybridization exists, which can be explained by the Kondo scattering with the thermally excited triplet crystalline electric field state. Our results help us to understand the intriguing properties in COS and POS, and provide a clean demonstration of the microscopic differences in heavy fermion systems with $4f^1$ and $4f^2$ configurations.

DOI: 10.1103/PhysRevLett.126.136402

Linking materials' properties to composition and structure is one of the central aims of materials research and, for strongly correlated materials, presents a long-standing challenge. A particularly rich class of materials where strong interactions play a decisive role is rare-earth intermetallic. At high temperatures the rare-earth electrons are localized and the interplay of electron localization vs itineracy at the various energies results in complex general phase diagrams with a wide range of possible ground states [1–3]. This interplay has been systematically studied in $CeTIn_5$ (T = transition metal). By tuning the conduction electrons through varying T among Co, Rh, and Ir, minute changes in the hybridization between conduction electrons and f electrons (c-f hybridization) lead to distinct ground states [4–6]. Alternatively, tuning the f electrons by replacing rare-earth elements also induces changes in physical properties [7–10], but the underlying systematics is hardly explored. In contrast to the intensively studied $4f^1$ system, even systematic experiments on the microscopic electronic behavior of $4f^2$ systems are scarce. The key problem on how the Kondo hybridization varies from $4f^1$ to $4f^2$ systems is yet to be settled.

Rare-earth compounds in filled-skutterudite structure (RT_4X_{12}, R = rare-earth compounds, X = pnictogen) offer an ideal playground in studying the Kondo physics with varied f electrons, which host various ground states and novel physical properties, including superconductivity [11], magnetism [12], non-Fermi liquid behavior [13,14], and semiconducting behavior [15–17]. Particularly, unconventional superconductivity with transition temperature of 1.86 K and Kondo insulating behavior with T_K around 90 K emerge out of the same lattice ROs_4Sb_{12}, in $PrOs_4Sb_{12}$ (POS) [11,18] and $CeOs_4Sb_{12}$ (COS) [15], respectively. Even after almost two decades of research, the presence of Kondo physics and the origin of the distinct ground states remain enigmatic. In POS, heavy fermion (HF) superconductivity was inferred from the large specific heat jump at superconductivity transition [18], the nodal superconducting gap [19–21], and the time reversal symmetry breaking [22]. The cyclotron effective mass measured by de Haas–van Alphen (dHvA), however, is only $2.4 \sim 7.6\, m_e$ [23], questioning the participation of f electrons in the ground states. The $4f^2$ ground state [24,25] and the nonmonotonic temperature dependence of the

effective mass [26] seem to contradict a conventional magnetic Kondo scenario. These exotic behaviors were suspected to involve extra degrees of freedom, e.g., like the quadrupolar fluctuations of the Pr 4 f electrons [24,27], whose effect on the electronic structure has not been identified. In contrast, COS in the $4f^1$ configuration hosts a ground state of antiferromagnetic (AFM) semiconducting phase with an enhanced effective mass [15]. The reported Kondo gap ranges from ~1 meV to 70 meV [15,28,29], which calls for further clarification via electronic structure measurements. Moreover, the theoretically proposed Fermi surface (FS) nesting [30,31] and nontrivial topological nature [32] in COS require a systematic investigation from an electronic structure perspective.

Angle-resolved photoemission spectroscopy (ARPES) has played a key role in studying the electronic structure in HF systems with layered structure [4–6,33,34]. In contrast, ARPES study on filled skutterdites is lacking so far, as their three-dimensional structure [Fig. 1(a)] poses significant challenges to surface sensitive ARPES studies. Here, combining the bulk sensitive soft x-ray (SX) ARPES and high resolution vacuum ultraviolet (VUV) ARPES studies, both with micrometer-sized beam spots (see Supplemental Material, Sec. I for experimental details [35]), we report the successful determination of the momentum dependent electronic structures of POS and COS, which directly reveals the distinctive interplay of localization and itineracy in $4f^1$ and $4f^2$ systems.

SX-ARPES measurements on POS reveal similar FSs in the k_x-k_z plane [Fig. 1(c)] and the equivalent k_x-k_y plane [Fig. 1(d)], consistent with the body-centered cubic structure, confirming the bulk origin of the measured bands. Along Γ-H, bands α and β cross the E_F [Fig. 1(e)], forming a hole pocket at Γ and an electron pocket at H, respectively [Fig. 1(d)]. Band δ around the N point has its band top barely touching E_F [Fig. 1(f)]. The VUV-ARPES data reveal a band structure that is distinct from the SX-ARPES data, implying the existence of surface states. Two electron bands η_1 and η_2 cross E_F near H [Fig. 1(g)], forming two elliptical pockets [Fig. 1(l)]. The 3D electronic structure of COS is generally identical to that of POS. As shown in Fig. 1(h), the FSs consist of a hole pocket (α) centered at Γ and an electron pocket (β) centered at H. The photoemission spectra along the high symmetry directions of Γ-H and Γ-N [Figs. 1(i)–1(j)] largely resemble those of POS. Moreover, surface states η_1 and η_2 are also observed around H with 102 eV photons in COS [Fig. 1(k)], which shows two-fold symmetry in the k_x-k_y plane (see Supplemental Material, Secs. II and III for details on extracting the bulk band dispersions, and determination of the surfaces states, respectively [35]). As summarized in Figs. 1(l)–1(n), COS and POS show similar FSs and bandwidth, indicating the same high-energy behavior in $R\mathrm{Os_4Sb_{12}}$.

To detect the f-electron behavior contributed by Pr (Ce) in POS (COS), we conducted resonant ARPES measurements at M and N edges of Pr (Ce) elements, whose

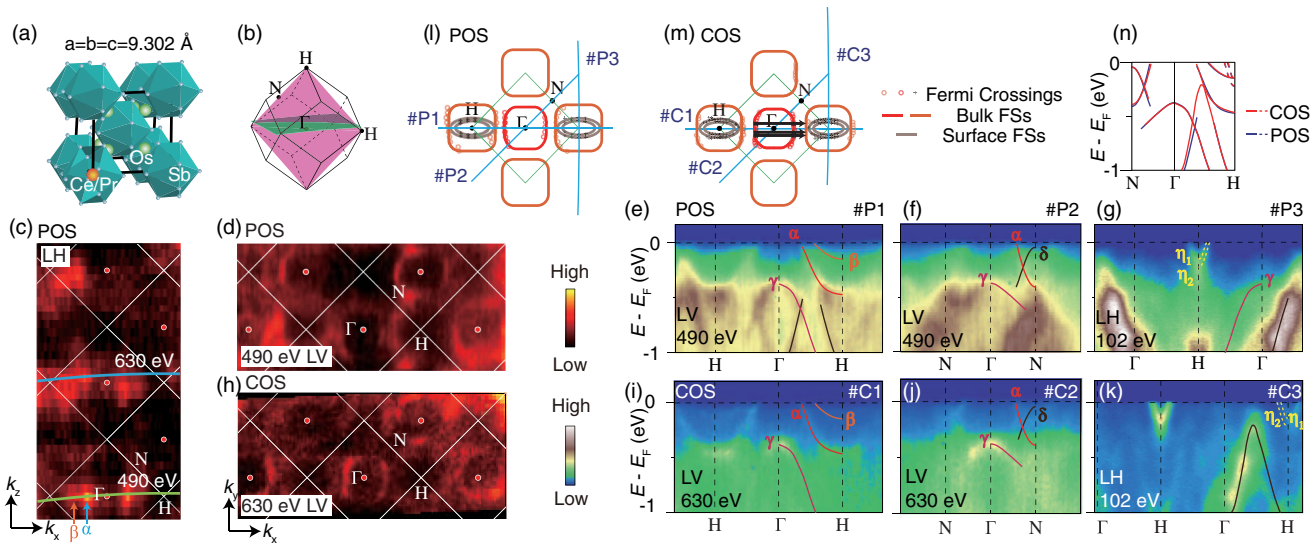

FIG. 1. (a) Crystal structure of the filled skutterudites. (b) Sketch of the Brillouin zone. The momentum spaces sampled in panels (c) (magenta), (d) and (h) (green) are illustrated. (c) SX-ARPES intensity map of POS integrated over $E_F \pm 100$ meV in the k_x-k_z plane, using 400 to 800 eV photons. The inner potential is estimated to be 15 eV. (d) SX-ARPES intensity map of POS in the k_x-k_y plane integrated over $E_F \pm 100$ meV, collected with 490 eV photons [green curve in panel (c)]. (e)–(g) Photoemission spectra of POS along cut P1, P2; and P3, respectively. (h) Same as panel (d) but for COS collected with 630 eV photons [blue curve in panel (c)]. (i)–(k) Same as (e)–(g), but of COS along cut C1, C2, and C3, respectively. (l) and (m) are the sketches of FSs and cuts for POS and COS, respectively. Fermi crossings were determined by local maxima in momentum distribution curves (MDCs). Black arrows indicate the proposed nesting vector close to (1,0,0) [30,31,36]. (n) Comparison of the band dispersions of POS and COS. Solid and dashed lines indicate bulk and surface states, respectively. SX-ARPES and VUV-ARPES data were taken at 19 K and 6.5 K, respectively.

energies were determined by x-ray absorption spectroscopy (XAS) measurements [35]. In POS, resonant enhancement of photoemission signals are observed near E_F and at binding energies (E_B) around 5 eV [Figs. 2(a) and 2(b)], which correspond to $4f^2$ final states and $4f^1$ final states, respectively [Fig. 2(c)] [37]. Considering the prominent Pr^{3+} valence in POS and the absence of the $4f^3$ initial state [38], the $4f^2$ final state comes from the photoemission process where the $4f$ photon hole at the $4f^1$ final state is immediately recombined by a conduction electron [39], and thus the detectable intensity of $4f^2$ final states indicates a nonvanishing c-f hybridization in POS. The participation of f electrons in the low-energy electronic states is consistent with the HF behavior in POS. The photoemission resonance peak of the $4f^2$ final states shows several sublevels [Figs. 2(g)–2(i)], whose energies can be well accounted for by the multiplets of the $4f^2$ configuration from theoretical calculations [37]. However, well-defined heavy-quasiparticle dispersion in the investigated temperature regime is absent [Fig. 2(h)].

In COS, resonant enhancements of photoemission signals are observed at $E_B = 3$ eV and near E_F, corresponding to the $4f^0$ and $4f^1$ final states, respectively [Figs. 2(d)–2(f)]. Unlike the similar resonance magnitude of Pr $4f^1$ and Pr $4f^2$ final states in POS, the resonance of Ce $4f^1$ near E_F is much stronger than the Ce $4f^0$. At the Ce 4 $d \rightarrow 4$ f resonant photon energy of 121.9 eV, resonant enhancements of two flat bands at E_F and $E_B = 0.25$ eV are resolved, corresponding to the Ce $4f^1_{5/2}$ and Ce $4f^1_{7/2}$ final states, respectively [Figs. 2(j)–2(l)]. The larger intensity ratio of $4f^1/4f^0$ in COS than that of $4f^2/4f^1$ in POS and the sharper heavy quasiparticle peaks observed in COS [Figs. 2(k) and 2(l)] indicate stronger c-f hybridization in COS. Ce $4f^1_{5/2}$ states in COS show a flat quasiparticle dispersion [Fig. 2(o)]. The holelike dispersion of the heavy band is distinct from the electronlike surface states. Moreover, the change of bulk band dispersion due to c-f hybridization can be clearly observed in the data taken with 200 eV photons without surface states (see Supplemental Material, Fig. S12 [35]), both suggesting that f electrons hybridize with bulk states rather than surface states. At E_F, the spectral weight of COS is enhanced at momenta inside the hole pocket α and outside the electron pocket β [Fig. 2(p)], and the flat band dispersion connects bulk bands α and β [Fig. 2(m)]. The hybridized band can be fitted to the mean field theory of the periodic Anderson model (PAM) as an effective low-energy model [40], and the effective energy dispersion can be given by $E^{\pm} = \{\varepsilon_f + \varepsilon(k) \pm \sqrt{[\varepsilon_f - \varepsilon(k)]^2 + 4|V_k|^2}\}/2$ where ε_f is the energy of the renormalized effective f level and $\varepsilon(k)$ is the dispersion of the bare band of conduction electrons. As shown by the resonant map (Supplemental Material,

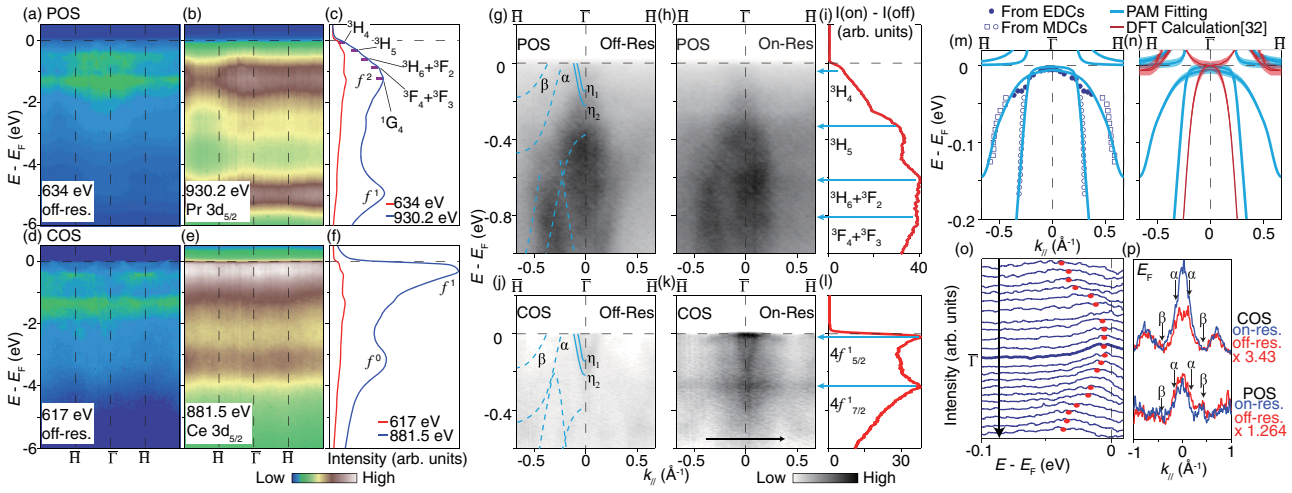

FIG. 2. (a)–(b) Photoemission spectra of POS taken at 19 K with Pr M edge off-resonance (634 eV) (a) and on-resonance (930.2 eV) photons (b), which are equivalent in the k_z periodicity. (c) Angle-integrated energy distribution curves (EDCs) of (a) and (b). (d)–(f), Same as (a)–(c), but measured on COS with Ce M edge off-resonance (617 eV) and on-resonance (881.5 eV) photons. (g),(h) Photoemission spectra of POS measured at 6.5 K with Pr N edge off-resonance (120.5 eV) and on-resonance (124.2 eV) photons, respectively. Dashed lines (not clear in this spectrum) and solid lines correspond to dispersions determined in Fig. 1. (i) The intensity difference of the EDCs integrated over the momentum range in panels (g) and (h). (j)–(l) The same as (g)–(i) but for COS samples near the Ce N edge with off-resonance (118 eV) and on-resonance (121.9 eV) photons. (m) Results of PAM fittings to COS illustrating the c-f hybridization. Blue circles and squares are obtained by fitting individual MDCs or EDCs (see Supplemental Material, Sec. V for extraction of band dispersions [35]). (n) A comparison between results of PAM fittings (blue) and calculation (red) with DFT including itinerant f states in Ref. [32]. Blue and red shadows stand for the spectral weight from Ce 4 f electrons. (o) EDCs along the arrow in panel (k) divided by the resolution convolved Fermi-Dirac function as a typical way to compensate for the cutoff near E_F by Fermi-Dirac distribution, showing the dispersion of the flat bands. (p) MDCs at E_F of the data shown in panels (g),(h) and (j),(k). Black arrows show the Fermi momenta of bands α and β.

Sec. VI [35]), the heavy band is observed below E_F at the BZ center, and thus PAM fitting along the high symmetric Γ-H direction gives the smallest gap. At 6.5 K, we find the f level near E_F and $|V_k|$ of 24 ± 6 meV for α and 28 ± 4 meV for β, corresponding to a direct gap of 48 ± 12 meV for α and 56 ± 8 meV for β, which are larger than that in $CeCoIn_5$ [4], suggesting stronger effective c-f hybridization in COS.

The formation of heavy quasiparticles in COS is revealed by temperature dependent ARPES measurements at the Ce N edge. The spectral weight of f states is not visible at 147 K [Fig. 3(f)]. At 13 K, a heavy band contributed by the c-f hybridized electrons is well developed [Fig. 3(a)], with an emerging peak near E_F in the integrated EDCs [Fig. 3(g)]. As the temperature decreases from 147 K to 13 K, the peak intensity increases smoothly, indicating the increasing c-f hybridization with no sharp transition [Fig. 3(i)]. Such a gradual formation of Kondo coherence is typical for HF systems [4–6,33,35] and Kondo insulators [41–44]. A gap opening due to c-f hybridization is observed [Fig. 3(h)], and the presence of a gap at low temperature due to c-f hybridization is repeatable on different samples [in Figs. 2(o) and 3(h)], accounting for the development of Kondo insulating behavior in COS at low temperature.

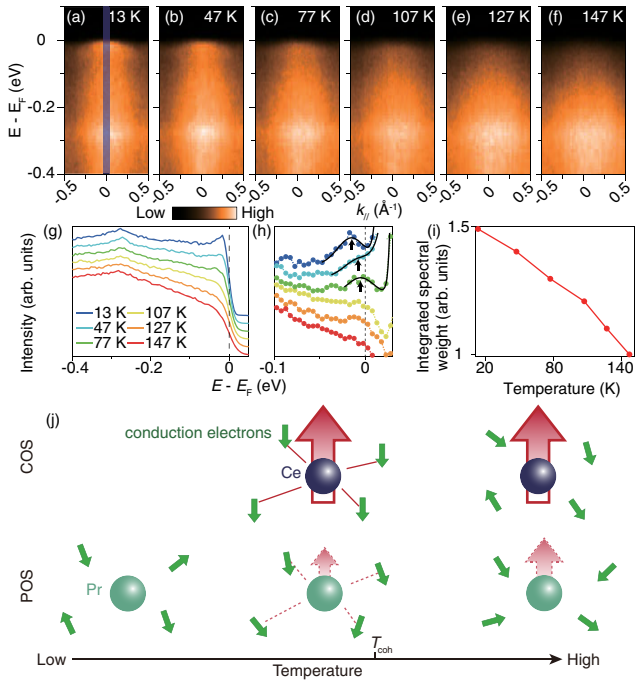

FIG. 3. (a)–(f) Resonant (121.6 eV, Ce N edge) photoemission spectra of another COS sample along $\bar{\Gamma}$-$\bar{H}$ at different temperatures. (g) EDCs integrated within the blue shaded area in (a) at different temperatures. (h) EDCs in (g) divided by the resolution convolved Fermi-Dirac function at corresponding temperatures. (i) Integrated spectral intensity over $[E_F - 0.1,\ E_F + 0.1\ \text{eV}]$, normalized by the intensity at 147 K. (j) Illustration of the magnetic Kondo screening in COS and POS evolving as a function of temperature. The green arrows indicate the spins of conduction electrons. The red arrows indicate the magnetic moments of Ce/Pr ions, with the size illustrating the average magnitude of the magnetic moments.

Our results reveal the distinctive features of conduction electrons interacting with $4f^1$ and $4f^2$ electrons. The observed electronic structure of POS and COS at the eV scale are strikingly similar, despite of the different rare-earth elements involved. Considering that the probed k_z of the resonant data in POS and COS are both close to the Γ-H-N plane, and that the sample quality in current studies would not prevent the observation of Kondo coherence (see Supplemental Material, Sec. VIII [35]), the different on-resonance data reflect the intrinsic difference in c-f hybridization. In COS, c-f hybridization is observed and gets coherent at low temperature [Fig. 3(a)], hallmarks of the Kondo screening of the Ce $4f^1$ local moment. In POS, the detection of the $4f^2$ final state in our experiments indicates the finite itineracy of Pr 4 f electrons and the presence of Kondo correlations. As the nonmagnetic singlet ground state in POS alone [45–48] cannot host a magnetic or quadrupole Kondo effect [46], crystalline electric field splitting should be considered.

As suggested by previous neutron scattering studies, just 0.7 meV above the Γ_1 ground state of Pr $4f^2$ lies a triplet magnetic state $\Gamma_4^{(2)}$, forming a Γ_1-$\Gamma_4^{(2)}$ pseudo-quartet [45,47–53]. Therefore, a fair amount of Pr atoms are thermally excited to the magnetic $\Gamma_4^{(2)}$ state at the measuring temperatures of ARPES studies which leads to magnetic moments at the Pr ions. Given that these temperatures are below typical T_{coh}, finite c-f hybridization exists through exchange interaction between itinerant electrons and thermally exited moments. Considering the large Van Vleck contribution in magnetic susceptibility [18,26], there should be a considerable weight of O_h triplet Γ_4 [54], favoring AFM over ferromagnetic interaction [54], leading to Kondo interaction in POS. The quadrupole degree of freedom interacting with conduction electrons through aspherical Coulomb scattering might also play a role in the incoherent hybridization, which calls for further theoretical investigations. With decreasing temperature, despite of the otherwise enhanced Kondo coherence and the magnetism from the intermediate state of hybridization, the prevailing factor is the diminishing participation of the magnetic $\Gamma_4^{(2)}$ triplet states. The competition between these effects would lead to a nonmonotonic strength of c-f hybridization as a function of temperature as illustrated in Fig. 3(j). This scenario is well consistent with the nonmonotonic behavior of cyclotron effective mass in previous nuclear magnetic resonance study with a maximum around 3 K [26] and the reduced mass in dHvA study at the extremely low temperature of 30 mK [23].

Our results also provide a microscopic basis for understanding the exotic properties in COS. (1) The quantitative

determination of Kondo gaps with momentum resolution helps us to understand the controversial gap sizes in previous reports [15,28,29]. Despite of the relatively large direct hybridization gap from PAM fitting [Fig. 2(m)], the indirect gap is of the order of 1 meV and the top of the hybridized band is only $\sim 8 \pm 5$ meV below the Fermi energy at Γ in the raw data [Fig. 2(o)]. The small indirect gap is compatible with the small gap ~1 meV determined by transport measurements [15], while the two direct gaps with band dependent sizes could explain the two-gap features at the order of 30 meV and 50 meV in previous neutron and optical conductivity studies [28,29]. The presence of the large direct gap and the small indirect gap explains the intriguing dual character of Kondo insulating behavior and HF behavior in COS at low temperature [15,55]. (2) Parallel FS sections are observed for the conduction electrons [Fig. 1(h)], which follows the nesting condition $q \sim (1, 0, 0)$ [black arrows in Fig. 1(m)] suggested as a driving force of the AFM ground state below 0.9 K [30,31,36]. Nevertheless, the nesting condition is no longer met at low temperature with the gapped electronic structure due to c-f hybridization, which brings us to the question of whether the spectral weight slightly below E_F, forming the remnant FSs, could play a role in driving antiferromagnetism. (3) A novel topological Kondo insulating state was proposed in COS by density-functional theory (DFT) calculations suggesting d-f band inversion near E_F [32]. However, the surface states are observed around H rather than Γ, in both COS and POS, which are topologically trivial, different from that in topological Kondo insulator SmB_6 [43]. It should be noted that the Kondo gap size in COS is rather small, comparable with the energy resolution of current ARPES techniques, which calls for future experiments with sub-meV energy resolution, such as STM-QPI studies, in fully ruling out the topological states. Despite the difficulty in examining the in-gap dispersion, the electronic structure revealed here poses constraints to theories. Clear discrepancies between the calculation and experimental electronic structure can be observed at the band bottom of H and the Kondo gap at Γ [Fig. 2(n)] (see Sec. IX in the Supplemental Material for details and a comparison with calculations in $LaOs_4Sb_{12}$ [35]). The measured band structure calls for a revision of the theoretical calculations with corrected band structure and the scrutiny of the d-f band inversion, which is a prerequisite for the formation of topological properties.

To summarize, we have experimentally revealed the band dispersions in filled-skutterudite COS and POS with different f electron configurations. There are striking differences between POS and COS in terms of their c-f hybridization, unveiling the development of Kondo insulating states in COS and the anomalous HF behavior in POS. These results provide a clean demonstration on how Kondo physics behaves differently in $4f^1$ and $4f^2$ configurations, causing drastically different ground states. Our work and methods will also motivate future ARPES studies on the filled-skutterudite family with various intriguing phenomena.

We gratefully acknowledge the experimental support of Dr. Y. B. Huang, Dr. P. Dudin, Dr. D. H. Lu, Dr. V. N. Strocov, and Dr. J. Denlinger. We thank the Diamond Light Source for access to beamline I05, the Shanghai Synchrotron Radiation Facility for access to beamline 09U, the Stanford Synchrotron Radiation Lightsource for access to beamline 5-2 and the Advanced Light Source for access to beamline 4.0.3. A. L. J. thanks J. Grin for continuous support. This work is supported in part by the National Key R&D Program of the MOST of China (Grants No. 2017YFA0303104, No. 2016YFA0300200, and No. 2017YFA0303004), Science Challenge Project (No. TZ2016004), the National Natural Science Foundation of China (Grants No. 11704073, No. U1630248, No. 11888101, No. 11922403, No. 11790310, and No. 11774307), Anhui Initiative in Quantum Information Technologies and Shanghai Municipal Science and Technology (Shanghai Rising-Star Program with Grant No. 20QA1401400, Major Project with Grant No. 2019SHZDZX01).

*xuhaichao@fudan.edu.cn
†pengrui@fudan.edu.cn
‡dlfeng@ustc.edu.cn

[1] S. Kawasaki, T. Mito, G.-q. Zheng, C. Thessieu, Y. Kawasaki, K. Ishida, Y. Kitaoka, T. Muramatsu, T. C. Kobayashi, D. Aoki, S. Araki, Y. Haga, R. Settai, and Y. Onuki, Phys. Rev. B **65**, 020504(R) (2001).
[2] P. Gegenwart, Q. Si, and F. Steglich, Nat. Phys. **4**, 186 (2008).
[3] S. Kirchner, S. Paschen, Q. Chen, S. Wirth, D. Feng, J. D. Thompson, and Q. Si, Rev. Mod. Phys. **92**, 011002 (2020).
[4] Q. Y. Chen *et al.*, Phys. Rev. B **96**, 045107 (2017).
[5] Q. Y. Chen, D. F. Xu, X. H. Niu, R. Peng, H. C. Xu, C. H. P. Wen, X. Liu, L. Shu, S. Y. Tan, X. C. Lai, Y. J. Zhang, H. Lee, V. N. Strocov, F. Bisti, P. Dudin, J. X. Zhu, H. Q. Yuan, S. Kirchner, and D. L. Feng, Phys. Rev. Lett. **120**, 066403 (2018).
[6] Q. Y. Chen, C. H. P. Wen, Q. Yao, K. Huang, Z. F. Ding, L. Shu, X. H. Niu, Y. Zhang, X. C. Lai, Y. B. Huang, G. B. Zhang, S. Kirchner, and D. L. Feng, Phys. Rev. B **97**, 075149 (2018).
[7] C. Petrovic, S. L. Budko, V. G. Kogan, and P. C. Canfield, Phys. Rev. B **66**, 054534 (2002).
[8] J. Hudis, R. Hu, C. L. Broholm, V. F. Mitrovic, and C. Petrovic, J. Magn. Magn. Mater. **307**, 301 (2006).
[9] Y. Isikawa, D. Kato, A. Mitsuda, T. Mizushima, and T. Kuwai, J. Magn. Magn. Mater. **272–276**, 635 (2004).
[10] E. L. Thomas, E. E. Erickson, M. Moldovan, D. P. Young, and J. Y. Chan, MRS Online Proc. Library **848**, 233 (2004).

[11] M. B. Maple, P. C. Ho, Z. V. S., N. A. Frederick, E. D. Bauer, W. M. Yuhasz, F. M. Woodward, and J. W. Lynn, J. Phys. Soc. Jpn. **71**, 23 (2002).
[12] E. D. Bauer, A. lebarski, N. A. Frederick, W. M. Yuhasz, M. B. Maple, D. Cao, F. Bridges, G. Giester, and P. Rogl, J. Phys. Condens. Matter **16**, 5095 (2004).
[13] M. Nicklas, S. Kirchner, R. Borth, R. Gumeniuk, W. Schnelle, H. Rosner, H. Borrmann, A. Leithe-Jasper, Y. Grin, and F. Steglich, Phys. Rev. Lett. **109**, 236405 (2012).
[14] R. E. Baumbach, P. C. Ho, T. A. Sayles, M. B. Maple, R. Wawryk, T. Cichorek, A. Pietraszko, and Z. Henkie, J. Phys. Condens. Matter **20**, 075110 (2008).
[15] E. D. Bauer, A. Slebarski, E. J. Freeman, C. Sirvent, and M. B. Maple, J. Phys. Condens. Matter **13**, 4495 (2001).
[16] H. Sugawara, S. Osaki, M. Kobayashi, T. Namiki, S. R. Saha, Y. Aoki, and H. Sato, Phys. Rev. B **71**, 125127 (2005).
[17] P. A. Venegas, F. A. Garcia, D. J. Garcia, G. G. Cabrera, M. A. Avila, and C. Rettori, Phys. Rev. B **94** (2016).
[18] E. D. Bauer, N. A. Frederick, P. C. Ho, V. S. Zapf, and M. B. Maple, Phys. Rev. B **65**, 100506(R) (2002).
[19] E. E. M. Chia, M. B. Salamon, H. Sugawara, and H. Sato, Phys. Rev. Lett. **91**, 247003 (2003).
[20] K. Izawa, Y. Nakajima, J. Goryo, Y. Matsuda, S. Osaki, H. Sugawara, H. Sato, P. Thalmeier, and K. Maki, Phys. Rev. Lett. **90**, 117001 (2003).
[21] K. Katayama, S. Kawasaki, M. Nishiyama, H. Sugawara, D. Kikuchi, H. Sato, and G.-q. Zheng, J. Phys. Soc. Jpn. **76**, 023701 (2007).
[22] Y. Aoki, A. Tsuchiya, T. Kanayama, S. R. Saha, H. Sugawara, H. Sato, W. Higemoto, A. Koda, K. Ohishi, K. Nishiyama, and R. Kadono, Phys. Rev. Lett. **91**, 067003 (2003).
[23] H. Sugawara, S. Osaki, S. R. Saha, Y. Aoki, H. Sato, Y. Inada, H. Shishido, R. Settai, Y. Onuki, H. Harima, and K. Oikawa, Phys. Rev. B **66**, 220504(R) (2002).
[24] M. Kohgi, K. Iwasa, M. Nakajima, N. Metoki, S. Araki, N. Bernhoeft, J.-M. Mignot, A. Gukasov, H. Sato, Y. Aoki, and H. Sugawara, J. Phys. Soc. Jpn. **72**, 1002 (2003).
[25] T. Tayama, T. Sakakibara, H. Sugawara, Y. Aoki, and H. Sato, J. Phys. Soc. Jpn. **72**, 1516 (2003).
[26] H. Tou, Y. Inaoka, M. Doi, M. Sera, K. Asaki, H. Kotegawa, H. Sugawara, and H. Sato, J. Phys. Soc. Jpn. **80**, 074703 (2011).
[27] K. Miyake, H. Kohno, and H. Harima, J. Phys. Condens. Matter **15**, L275 (2003).
[28] M. Matsunami, H. Okamura, T. Nanba, H. Sugawara, and H. Sato, J. Phys. Soc. Jpn. **72**, 2722 (2003).
[29] D. T. Adroja, J. G. Park, E. A. Goremychkin, K. A. McEwen, N. Takeda, B. D. Rainford, K. S. Knight, J. W. Taylor, J. Park, H. C. Walker, R. Osborn, and P. S. Riseborough, Phys. Rev. B **75**, 014418 (2007).
[30] Y. Imai, K. Sakurazawa, and T. Saso, J. Phys. Soc. Jpn. **75**, 033706 (2006).
[31] Y. Imai and T. Saso, Phys. Rev. B **75**, 165102 (2007).
[32] B. Yan, L. Muchler, X.-L. Qi, S.-C. Zhang, and C. Felser, Phys. Rev. B **85**, 165125 (2012).
[33] Q. Yao, D. Kaczorowski, P. Swatek, D. Gnida, C. H. P. Wen, X. H. Niu, R. Peng, H. C. Xu, P. Dudin, S. Kirchner, Q. Y. Chen, D. W. Shen, and D. L. Feng, Phys. Rev. B **99**, 081107(R) (2019).
[34] H. J. Im, T. Ito, H. D. Kim, S. Kimura, K. E. Lee, J. B. Hong, Y. S. Kwon, A. Yasui, and H. Yamagami, Phys. Rev. Lett. **100**, 176402 (2008).
[35] See Supplemental Material at http://link.aps.org/supplemental/10.1103/PhysRevLett.126.136402 for detailed information.
[36] C. P. Yang, H. Wang, J. F. Hu, K. Iwasa, M. Kohgi, H. Sugawara, and H. Sato, J. Phys. Chem. C **111**, 2391 (2007).
[37] H. Ishii, T. Miyahara, Y. Takayama, K. Obu, M. Shinoda, C. Lee, H. Shiozawa, S. Yuasa, T. D. Matsuda, H. Sugawara, and H. Sato, Surf. Rev. Lett. **09**, 1257 (2002).
[38] D. Cao, F. Bridges, S. Bushart, E. D. Bauer, and M. B. Maple, Phys. Rev. B **67**, 180511 (2003).
[39] S. Hufner, *Photoelectron Spectroscopy: Principles and Applications* (Springer Science & Business Media, New York, 2013).
[40] A. C. Hewson, *The Kondo Problem to Heavy Fermions* (Cambridge University Press, Cambridge, England, 1997), Vol. 2.
[41] S. Seong, K. Kim, E. Lee, C.-J. Kang, T. Nam, B. I. Min, T. Yoshino, T. Takabatake, J. D. Denlinger, and J. S. Kang, Phys. Rev. B **100** (2019).
[42] N. Xu, C. E. Matt, E. Pomjakushina, X. Shi, R. S. Dhaka, N. C. Plumb, M. Radovic, P. K. Biswas, D. Evtushinsky, V. Zabolotnyy, J. H. Dil, K. Conder, J. Mesot, H. Ding, and M. Shi, Phys. Rev. B **90**, 085148 (2014).
[43] J. Jiang, S. Li, T. Zhang, Z. Sun, F. Chen, Z. R. Ye, M. Xu, Q. Q. Ge, S. Y. Tan, X. H. Niu, M. Xia, B. P. Xie, Y. F. Li, X. H. Chen, H. H. Wen, and D. L. Feng, Nat. Commun. **4**, 3010 (2013).
[44] Y. Takeda, M. Arita, M. Higashiguchi, K. Shimada, H. Namatame, M. Taniguchi, F. Iga, and T. Takabatake, Phys. Rev. B **73**, 033202 (2006).
[45] S. Raymond, K. Kuwahara, K. Kaneko, K. Iwasa, M. Kohgi, A. Hiess, M. A. Measson, J. Flouquet, N. Metoki, H. Sugawara, H. Aoki, and H. Sato, J. Phys. Soc. Jpn. **77**, 25 (2008).
[46] E. A. Goremychkin, R. Osborn, E. D. Bauer, M. B. Maple, N. A. Frederick, W. M. Yuhasz, F. M. Woodward, and J. W. Lynn, Phys. Rev. Lett. **93**, 157003 (2004).
[47] K. Kuwahara, K. Iwasa, M. Kohgi, K. Kaneko, S. Araki, N. Metoki, H. Sugawara, Y. Aoki, and H. Sato, J. Phys. Soc. Jpn. **73**, 1438 (2004).
[48] K. Kuwahara, K. Iwasa, M. Kohgi, K. Kaneko, N. Metoki, S. Raymond, M. A. Measson, J. Flouquet, H. Sugawara, Y. Aoki, and H. Sato, Phys. Rev. Lett. **95**, 107003 (2005).
[49] Y. Aoki, T. Tayama, T. Sakakibara, K. Kuwahara, K. Iwasa, M. Kohgi, W. Higemoto, D. E. MacLaughlin, H. Sugawara, and H. Sato, J. Phys. Soc. Jpn. **76**, 051006 (2007).
[50] R. Shiina, M. Matsumoto, and M. Koga, J. Phys. Soc. Jpn. **73**, 3453 (2004).

[51] K. Kuwahara, K. Iwasa, M. Kohgi, K. Kaneko, N. Metoki, S. Raymond, M. A. Masson, J. Flouquet, H. Sugawara, Y. Aoki, and H. Sato, Physica (Amsterdam) **385–386B**, 82 (2006).

[52] P. Fazekas, *Lecture Notes on Electron Correlation and Magnetism* (World Scientific, Singapore, 1999), Vol. 5.

[53] U. Walter, Z. Phys. B **62**, 299 (1986).

[54] J. Otsuki, H. Kusunose, and Y. Kuramoto, J. Phys. Soc. Jpn. **74**, 200 (2005).

[55] M. Matsunami, R. Eguchi, T. Kiss, K. Horiba, A. Chainani, M. Taguchi, K. Yamamoto, T. Togashi, S. Watanabe, X. Y. Wang, C. T. Chen, Y. Senba, H. Ohashi, H. Sugawara, H. Sato, H. Harima, and S. Shin, Phys. Rev. Lett. **102**, 036403 (2009).